Hindawi Publishing Corporation
EURASIP Journal on Wireless Communications and Networking
Volume 2006, Article ID 40380, Pages 1–13
DOI 10.1155/WCN/2006/40380

Interference Mitigation for Coexistence of Heterogeneous Ultra-Wideband Systems

Yongjing Zhang,[1] Haitao Wu,[2] Qian Zhang,[3] and Ping Zhang[1]

[1] *Beijing University of Posts and Telecommunications, China*
[2] *Microsoft Research Asia, Beijing, China*
[3] *Hong Kong University of Science and Technology, Hong Kong*

Received 29 August 2005; Revised 9 January 2006; Accepted 3 April 2006

Two ultra-wideband (UWB) specifications, that is, direct-sequence (DS) UWB and multiband-orthogonal frequency division multiplexing (MB-OFDM) UWB, have been proposed as the candidates of the IEEE 802.15.3a, competing for the standard of high-speed wireless personal area networks (WPAN). Due to the withdrawal of the standardization process, the two heterogeneous UWB technologies will coexist in the future commercial market. In this paper, we investigate the mutual interference of such coexistence scenarios by physical layer Monte Carlo simulations. The results reveal that the coexistence severely degrades the performance of both UWB systems. Moreover, such interference is asymmetric due to the heterogeneity of the two systems. Therefore, we propose the goodput-oriented utility-based transmit power control (GUTPC) algorithm for interference mitigation. The feasible condition and the convergence property of GUTPC are investigated, and the choice of the coefficients is discussed for fairness and efficiency. Numerical results demonstrate that GUTPC improves the goodput of the coexisting systems effectively and fairly with saved power.

1. INTRODUCTION

In recent years, two novel ultra-wideband (UWB) technologies, that is, multiband-orthogonal frequency division multiplexing (MB-OFDM) UWB and direct-sequence (DS) UWB, have been proposed to IEEE 802.15.3a task group (TG3a) as the higher-speed physical (PHY) technology for next generation wireless personal area networks (WPAN). The two technologies are incompatible and can be treated as heterogeneous radio: MB-OFDM UWB adopts OFDM technology in a single band for high frequency efficiency and uses frequency hopping (FH) across multiple subbands for frequency diversity, while DS UWB is based on direct sequence spread spectrum (DSSS) technology over the whole band to support fairly high data rate. After three years of discussions without a decision being reached, the members of TG3a have to vote to withdraw the UWB standardization process, whereas the two UWB support camps, UWB Forum and WiMedia Alliance, have issued a joint statement that "the industry will continue to grow the UWB market" [1]. Thus, the coexistence of the two UWB devices becomes unavoidable in the near future. Since the channel allocation in the mandatory mode (see Section 2) of MB-OFDM and DS UWB systems occupies the same frequency band (3.1–4.8 GHz) and the bandwidth of the two system is extremely wide (about 1.5 GHz), it is hard to avoid frequency overlapping when the two systems coexist.

Many works [2–6] have investigated the issue about radio coexistence with UWB involved. However, most works assume UWB as impulse radio, which is different from both MB-OFDM and DS UWB technologies, and the victim systems are usually the legacy narrowband systems such as 802.11, GSM, and GPS. In [7, 8], MB-OFDM UWB is investigated as the interferer, while victims are legacy narrowband system and the impulse UWB, respectively. Therefore, all the existing work cannot be used to analyze the interference between MB-OFDM and DS UWB systems.

We implement the system models closely following the definition in MB-OFDM and DS UWB specifications. Based on the verified system models, the performance of DS and MB-OFDM systems under each other's interference is examined in coexistence scenarios. The results show that the coexistence of the two UWB systems degrades both systems' performance significantly, while the mutual impact is asymmetric due to the different system design. The degraded performance motivates us to propose a transmit power control algorithm to mitigate the interference between these two heterogeneous UWB systems.

Comparing with power control algorithms in related work, the one for heterogeneous UWB systems has its unique challenges. Firstly, information exchange is unlikely applicable between the two coexisting systems, which are unaware of the situation experienced at the other, due to incompatible PHY technologies. Secondly, the network structure composed by the coexisting systems is decentralized, which is different from the case in centralized cellular network such as in [9]. Thirdly, the heterogeneity between the coexisting systems leads to asymmetric system performance degradation, which brings new challenge to achieve fairness when designing power control algorithm.

In this paper, the goodput-oriented utility-based transmit power control (GUTPC) algorithm is proposed for mitigating interference caused by coexistence of heterogeneous UWB systems. Our intention is to improve the performance of the coexisting systems fairly by maximizing their net utilities, where the gain is as the goodput achieved, while the cost is as the power used and the signal-to-interference-and -noise ratio (SINR) observed. The SINR-based pricing function is novel and is proposed to achieve fairness adaptively. Under the generalized feasibility conditions of GUTPC, its convergence is proved by resorting to the *standard power control* [10] theorems. Considering that the coexisting systems may be turned off due to severe interference, we select the pricing coefficients fairly under the proposed *turn-off fairness* criterion (details will be given in Section 4), which deals with the performance gap between the heterogeneous systems. As shown in the numerical results, GUTPC is effective in interference mitigation for coexisting heterogeneous UWB systems and it approximates the *proportional fair* outcomes under *turn-off fairness* criterion with the optimal pricing coefficient.

The rest of this paper is organized as follows. Section 2 describes the PHY models of the coexisting UWB systems. In Section 3, we analyze the mutual-interference effects by Monte Carlo simulations, and the results are filtered with our proposed model. Section 4 proposes our power control algorithm, GUTPC, and investigates its feasibility and convergence properties as well as the choice of the pricing coefficient. The performance of GUTPC is evaluated in Section 5. Finally, the paper is concluded in Section 6.

2. SYSTEM MODELING

We implement the transmitters of the MB-OFDM UWB and DS UWB closely following their PHY specifications [11, 12], and design the receivers according to some references [13–21] since the implementations of receivers are not specified and flexible depending on the complexity. Both systems are constructed using the equivalent baseband model with perfect timing and frequency synchronization. Without losing generality, we choose the mandatory mode of each system and verify the system performance by comparing the evaluation results to references.

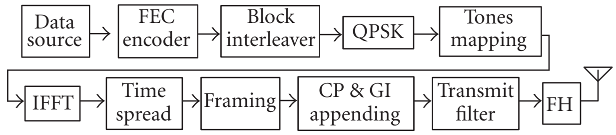

(a) MB-OFDM UWB transmitter implementation

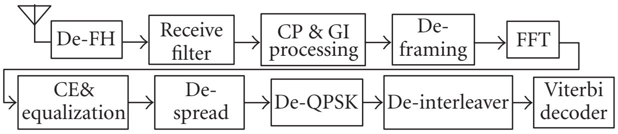

(b) MB-OFDM UWB receiver implementation

Figure 1

2.1. MB-OFDM UWB system

According to [11], the mandatory mode of MB-OFDM system is operating in band group 1 (3.168–4.752 GHz) which consists of 3 adjacent bands. Each band can hold an OFDM symbol of 128 subcarriers, occupying 528 MHz spectrum. Over the 3 bands, FH is adopted based on the pattern defined by the time-frequency code. The structures of the transmitter and the receiver are shown in Figure 1.

The forward error correction (FEC) encoder is implemented by puncturing the outcome of the convolutional encoder. Correspondingly, an unquantized soft-decision Viterbi decoder is adopted in the receiver because float-point operation is used in our simulations. To achieve intersymbol and intrasymbol interleaving, 2-stage block interleaving is adopted. Before IFFT transformation, the guard tones are appended to each symbol as the copies of the "outmost" data tones [13] for certain diversity gain. Correspondingly, they are combined at the receiver by maximum-ratio combing. Time spread may be needed (e.g., at 200 Mbps) for payload symbols. As an OFDM system, guard interval (GI) and cyclic prefix (CP) are necessary for each symbol to overcome the intercarrier interference (ICI). According to [14–16], we implement CP as zero padding to avoid ripples in spectrum while keeping the same multipath robustness. Further, to mitigate intersymbol interference (ISI), channel estimation (CE) and equalization are performed in frequency domain with the help of CE training sequence in the preamble.

2.2. DS UWB system

According to [12], the mandatory mode of DS system is operating in channel 1–4 (3.1–4.85 GHz) with binary phase shift keying (BPSK) modulation. The structures of the transmitter and the receiver are shown in Figure 2.

The FEC encoding/decoding is similar to that of MB-OFDM system, whereas the interleaving is achieved by convolutional interleaving. Different length of ternary spread codes is used for data spreading and generating the acquisition sequence (AS) and training sequence (TS) in the preamble [12, 17]. To overcome the multipath channel fading we adopt the RAKE [20] algorithm in the receiver and

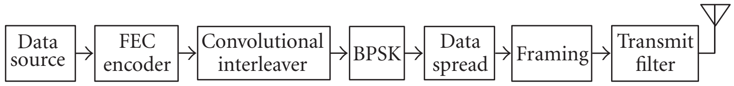

(a) DS UWB transmitter implementation

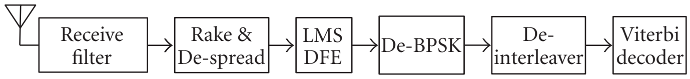

(b) DS UWB receiver implementation

Figure 2

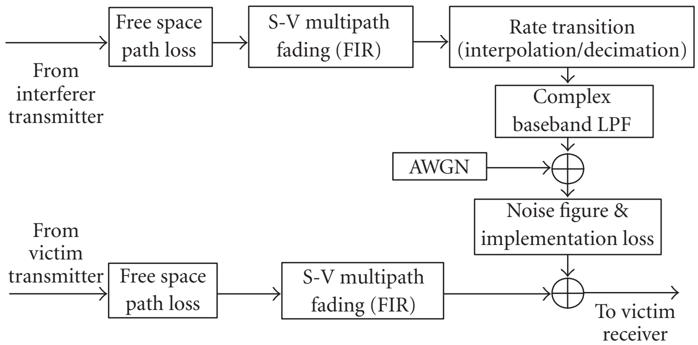

Figure 3: UWB coexistence channel model implementation.

implement it as a 16-finger finite impulse response (FIR) filter [17–19], of which the coefficients are trained by the received AS. After that, a 31-tap sample-spaced decision feedback equalizer (DFE) [17, 19] is introduced to deal with ISI. Due to the time-invariant characteristic of the UWB channel model (see Section 2.3), the least-mean-square (LMS) algorithm is employed in the DFE for its low complexity and is trained by TS for each received PHY frame.

Besides, there should be practically 6.6 dB noise figure at the receiver front-end and also 2.5 dB (in case of 200 Mbps) implementation loss in the receivers of both UWB systems according to [11, 18, 19, 21]. We incorporate these degradation factors in the channel model as detailed next.

2.3. Channel model

We construct the UWB channel following the final report [22] from the channel modeling subcommittee of IEEE 802.15. Both the path loss model and the multipath model are implemented in our simulations.

The path loss model is a free space model which can be formulated (in dB) as

$$P_r = P_t + G_t + G_r - 20\log\left(\frac{4\pi f_c'}{c}\right) - 20\log(d), \qquad (1)$$

where P_t is the transmit power, G_t and G_r are the antenna gains (considered as zeros) at the transmitter and receiver, respectively, c is the speed of light (3×10^8 m/s), d is the distance, f_c' is the geometric center frequency of waveform [22], and P_t is set to -9.9 dBm in both UWB systems [13, 21].

The multipath model is a stochastic tapped-delay-line channel model derived from the Saleh-Valenzuela model with minor modifications. It includes four subtypes as channel model 1–4 (denoted by CM1–CM4) and we build our work on the line-of-sight CM1 channel using an FIR filter. The filter's coefficients are achieved by resampling and down-converting the original "continuous time" channel realizations according to the required sample rate and center frequency of each UWB system. Besides, the time variability is not considered in [22] due to the lack of empirical data, so the channel is assumed to be time invariant.

The coexisting channel model is implemented through combining the useful signal, noise, and interference as shown in Figure 3. To align the sample rates of the coexisting systems, we apply a decimator/interpolator before injecting the interfering signal into the useful signal of the victim. Additionally, a complex baseband filter is cascaded to avoid frequency aliasing while keeping the relative offset of the center frequencies of the two systems. As mentioned before, we incorporate the noise figure and the implementation loss of the receivers as the increment of the noise floor, that is, the sum of the additional white Gaussian noise (AWGN) and the interference.

2.4. System performance self-evaluation

Based on the system modeling described above, we first verify the performance of the two UWB systems in AWGN and CM1 channels without mutualinterference. As for the CM1 channel, the performance in the 90th percentile (10%

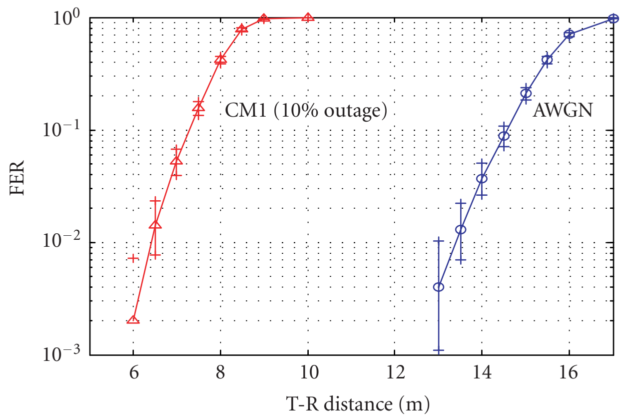

(a) MB-OFDM UWB (200 Mbps) performance

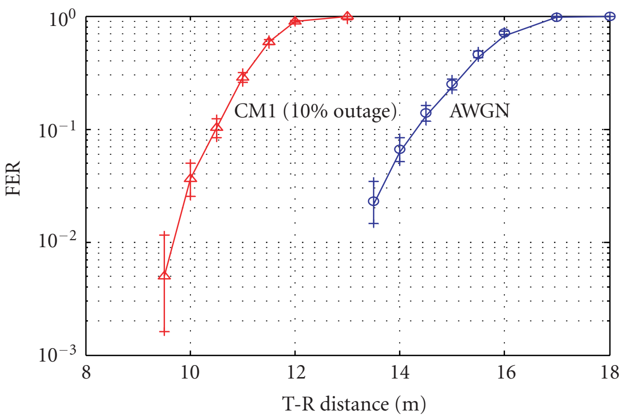

(b) DS UWB (220 Mbps) performance

Figure 4

outage) channel realization is evaluated. Here we set MB-OFDM UWB operating at 200 Mbps in band group 1 and DS UWB operating at 220 Mbps in channel 4 as examples. Note that the chosen data rates of the two systems are slightly different since their available rate sets are not quite compatible. The criterion is the maximum transmitter-receiver (T-R) distance to achieve 8% PER with 1 kbyte payload size [23]. The Monte Carlo simulation results with the 95% confident interval are shown in Figure 4.

As for MB-OFDM system, the required PER (8%) can be achieved at the T-R distance of at most 14.3 m in AWGN channel. This distance is reduced to 7.2 m in CM1 channel due to the serious multipath effects. When it comes to DS system, the required PER can be achieved at 14.1 m and 10.3 m in AWGN and CM1 channels, respectively. From these results we observe that the performances of the two systems in AWGN channel are quite similar, while DS UWB outperforms MB-OFDM UWB much in CM1 channel. This could be explained as DS system has relatively wider bandwidth and processes the signal coherently over the whole bandwidth, which captures the full benefits of UWB propagation [24]. The results are also consistent with the related references [11, 13, 19, 21].

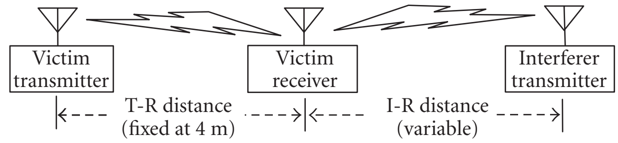

Figure 5: UWB coexistence scenario.

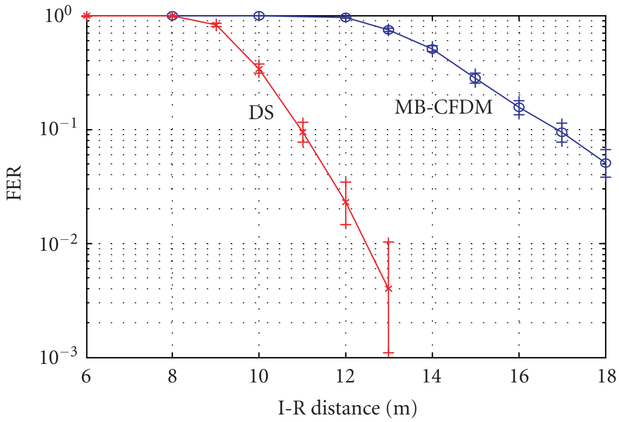

Figure 6: Coexistence performance in CM1 channel.

3. INTERFERENCE ANALYSIS

Through PHY Monte Carlo simulations, in this section, serious mutual interference of the two systems is demonstrated. By fitting the simulation results to performance curves, we propose a generalized model of the mean PER for the given coexisting systems. We observe that power control could be an effective approach to improve the performance of the two heterogeneous UWB systems on their coexistence.

3.1. Simulation results

Taking the same system parameters as in Section 2.4, we focus on the scenario that contains one interferer node (only transmitter) and one victim link (both transmitter and receiver) for simplicity as shown in Figure 5. The T-R distance of the victim is fixed at 4 m, which is the expected working distance for the data rate about 200 Mbps [23]. Correspondingly, the "I-R distance" denotes the distance between the interferer's transmitter and the victim's receiver. The evaluation criterion is the minimum I-R distance required by the victim to achieve 8% PER with 1 kbyte payload size. The transmitters of both the victim and the interferer keep transmitting packets continuously ignoring detailed MAC behaviors. The simulation results for mutual interference of the two systems with 95% confident interval are depicted in Figure 6.

Firstly, from the performance of MB-OFDM UWB under the interference of DS, we observe that the I-R distance should be at least 17.2 m to guarantee the victim 8% PER for communications. It means that to ensure MB-OFDM (200 Mbps) system working properly at the nominal T-R distance of 4 m, the interfering DS transmitter should be put

17.2 m away from the MB-OFDM receiver. It is a quite pessimistic result that a MB-OFDM system is vulnerable to a DS interferer coexisting within an indoor environment. Secondly, the DS UWB performance under the interference of MB-OFDM is still pessimistic in that the I-R distance should be at least 11.1 m to achieve the same criterion. It also reveals that the DS system outperforms the MB-OFDM system in the coexistence scenarios due to the less endurance of MB-OFDM UWB under the multipath environment, which is consistent with the performance evaluation in Section 2.4.

Hence we conclude that the I-R distance requirement is hard to achieve in practical indoor environment, thereby certain mitigation methods must be provided for the coexistent operation of these two UWB systems.

3.2. Coexisting model generalization

To design an effective interference mitigation method, we seek a generalized coexisting model to investigate the system performance under various situations. Since PER requirement is the basic performance criterion, the coexisting model is generalized as the mean PER expression based on the available system parameters (e.g., transmit power, T-R/I-R distance, and packet length). To achieve it, we derive the mean bit error rate (BER) by fitting the simulation results into the parameterized BER function. Finally, the proposed model is verified by further simulations.

Assuming that the bit errors are independent and the packet length (k, in bits) is fixed, the mapping relationship between the mean PER (P_p) and the mean BER (P_b) is

$$P_p = 1 - \left(1 - P_b\right)^k. \quad (2)$$

Usually the BER is determined by the received SINR if interference is introduced noncorrelatively, which stands in our coexistence problem since the coexisting UWB systems use totally different technologies and transmit randomized data. According to [20], the BER of a digital phase-modulated (e.g., QPSK and BPSK as in MB-OFDM and DS systems, resp.) signals in the AWGN channel follows the form as

$$P_b = \frac{1}{2}\,\mathrm{erfc}\left(\frac{\sqrt{E_b/N_0}}{\beta}\right), \quad (3)$$

where E_b is the signal energy per bit, N_0 is the noise PSD, β is a constant corresponding to different modulation method and signal correlation, and $\mathrm{erfc}(\cdot)$ is the complementary error function.

As for the time-invariant multipath channel (i.e., CM1) in this study, we can derive the mean BER function of both UWB systems by parameterizing (3) as

$$P_b = \frac{1}{2}\,\mathrm{erfc}\left(\frac{\left(\gamma_b\right)^{1/\alpha}}{\beta}\right), \quad (4)$$

where γ_b denotes the effective SINR per bit corresponding to E_b/N_0 in (3) while considering channel coding and the receiver impairments, α is a modified factor for CM1 channel. Given the channel and the system modulation parameters, there will be a unique pair of α and β that determine the BER performance versus γ_b.

Table 1: System parameters for PER curve fitting.

	DS (channel 4)	MB-OFDM (band group 1)
Data rate (R_b)	220 Mbps	200 Mbps
Two-side bandwidth (B)	1352 MHz	1584 MHz
Center frequency (f_c)	4056 MHz	3960 MHz
AWGN PSD (N_0)	−174 dBm/Hz	
Packet length (k)	1024*8 bits	
Transmit power (P_U, P_I)	−9.9 dBm	
T-R distance (d_U)	4 m	
Coupled power factor (η)	0.94	
α	1.99	2.22
β	0.74	1.05

Moreover, we have the SINR formulation with respect to the useful signal transmit power (P_U), the interfering signal transmit power (P_I) as

$$\gamma_b = \frac{P_U h_U}{\left(P_I h_I \eta\left(R_b/B\right) + N_0 R_b\right)L}, \quad (5)$$

where h_U and h_I are the path loss of the useful signal and the interfering signal, respectively, following (1), R_b and B are the data rate and the two-side bandwidth of the victim system, η is an approximate coupled power factor due to the slight offset between the central frequencies of the two systems, and L is the noise increment due to the receiver noise figure and implementation loss as mentioned before.

Thus, with the simulation results obtained and the parameters listed in Table 1, we can get the corresponding P_b and γ_b following (2) and (5), respectively. By substituting the P_b and γ_b into (4), the parameter α and β can be obtained as in Table 1 by curve fitting. Consequently we have the unique formula of mean PER as

$$P_p = 1 - \left(1 - \frac{1}{2}\,\mathrm{erfc}\left(\frac{1}{\beta}\left(\gamma_b\right)^{1/\alpha}\right)\right)^k. \quad (6)$$

Based on (5) and (6), we can easily extend the performance curves to various cases to help evaluate the possible effects of any interference mitigation method. Specifically, under given packet length, the coexistence topology and the data rate of each system, the PER is uniquely determined by P_U and P_I. By setting different P_I at −4 dB step (which is required in DS specification [12] for power control), we illustrate the estimated PER of both DS and MB-OFDM UWB systems along with the corresponding simulation results in Figure 7. It can be seen that the effect of power control is significant that when P_I reduces a few steps, the coexistence distance can be greatly shortened for the same required PER observed at the victim. Therefore, we conclude that power control is a promising interference mitigation method for coexistence of the two UWB systems, and the deduced model in (6) is appropriate for the coexistence analysis and for the power control algorithm design in the next section.

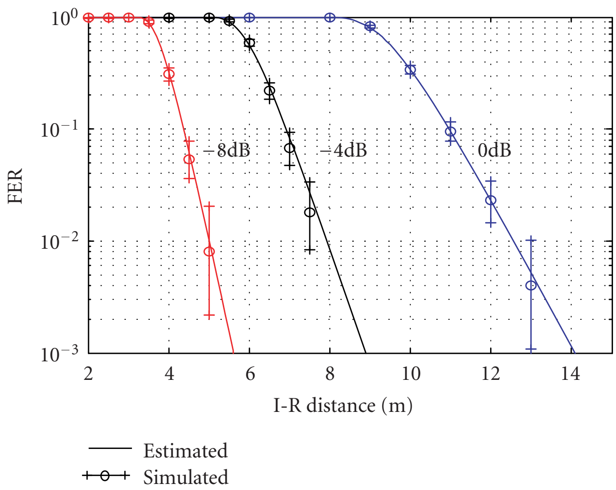

(a) DS performance with different interfering power

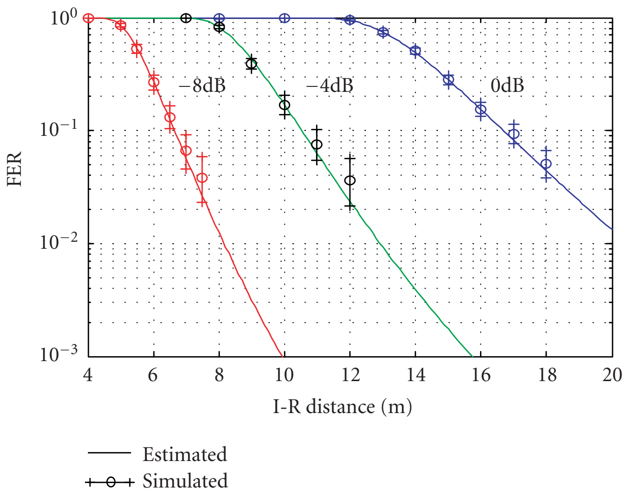

(b) MB-OFDM performance with different interfering power

Figure 7

4. POWER CONTROL FOR INTERFERENCE MITIGATION

Motivated by the simulation and analysis results above, we take power control as the interference mitigation approach for the coexistence problem of MB-OFDM UWB and DS UWB. In this paper, the target is a transmit power control (TPC) algorithm that improve the total goodput of the two coexisting UWB systems in a fair way. Considering that the information exchange is unlikely applicable between the heterogeneous coexisting UWB systems, a decentralized goodput-oriented utility-based TPC (GUTPC) algorithm is proposed. The feasible condition of GUTPC is investigated considering maximum power constraint, and the convergence is proved by resorting to the *standard power control* theorems. At last, we discuss the choice of the pricing coefficient under GUTPC based on the proposed *turn-off fairness* criterion.

4.1. Problem formulations

We propose GUTPC to improve the total goodput of the coexisting systems by each system maximizing its own net utility via tuning transmit power noncooperatively. The selection of the net utility function is critical and we formulate it as the combination of goodput and SINR-based price in GUTPC. Meanwhile, the heterogeneity between the coexisting systems is considered by distinguishing the pricing coefficients for the sake of fairness.

Being a goodput-oriented algorithm, the utility could be naturally chosen as the goodput function. However, it makes all greedy nodes transmit at the maximal power in that higher power always yields higher SINR, thus higher goodput from the local view of each node. This *Nash equilibrium*, though is *Pareto optimal* (by [9, Theorem 1]) from a game theory point of view, may lead to great performance degradation caused by severe interference between the coexisting systems. Thus, a pricing mechanism is necessary to shape the nodes to behave more efficiently from the global point of view. Accordingly, we formulate GUTPC as follows.

Let $\mathbf{p}$ denote the power vector of all links, let p_i denote the transmit power of link i, then the net utility function $U_i(\mathbf{p})$ of link i under GUTPC is

$$U_i(\mathbf{p}) = V_i(\mathbf{p}) - C_i(p_i), \tag{7}$$

where $V_i(\mathbf{p})$ and $C_i(p_i)$ are the goodput and pricing function of link i, respectively.

The goodput results from the successful packet transmission under given link capacity (i.e., the maximum achievable data rate), thus we have

$$V_i(\mathbf{p}) = R_i f_i(\mathbf{p}), \tag{8}$$

where R_i is the link capacity and $f_i(\mathbf{p})$ is the packet successful rate written as

$$f_i(\mathbf{p}) = 1 - P_p, \tag{9}$$

where P_p is the PER following (6).

Since $V_i(\mathbf{p})$ is inherently determined by the coexisting systems, the design of $C_i(p_i)$ is crucial for the net utility function. Basically, $C_i(p_i)$ should be an increasing function of p_i to charge the nodes for their transmit power in terms of radio resources usage. A classical approach [25, 26] is the linear form as

$$C_i(p_i) = \tau_i p_i, \tag{10}$$

where τ_i is a constant pricing coefficient.

However, when fairness is taken into account, a simple coefficient τ_i is not sufficient for the coexistence scenarios, because the network topology could be more complex than the single-cell cellular case as in [9, 25, 26] and the coexisting systems differ greatly in their goodput performance.

When considering the network topology, the physical position determined by the T-R and I-R distances usually is not easy to get in a practical system. Instead, the T-R path loss and the interference level are measurable in terms of the received power by the coexisting systems, thus can be used for

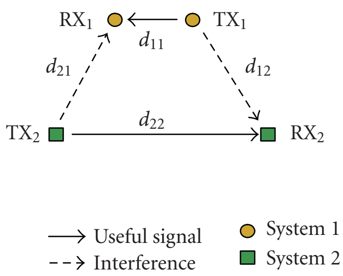

(a) Same interference power, different path loss

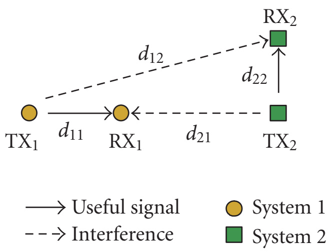

(b) Same path loss, different interference power

Figure 8

the pricing in power control [25]. However, the unilateral use of either of them may bring improper evaluation. We illustrate this problem using the examples in Figure 8, assuming that the two pairs of coexisting systems transmit at the same power.

Firstly, the interference level cannot reflect the unfairness caused by asymmetric T-R distances. In Figure 8(a), the coexisting systems cause the same interference to each other since they have the same I-R path loss resulted from the same I-R distance ($d_{12} = d_{21}$). However, the useful signal power received by the two systems differs greatly because of different T-R distance ($d_{22} > d_{11}$). Thus, system 1 has higher SINR and correspondingly higher performance than system 2 under this condition. Therefore, system 1 has higher potentiality to reduce its transmit power to improve the performance of system 2, while keeping its own performance acceptable. Accordingly, system 1 should be priced more than system 2 in this case for fairness and overall efficiency.

Secondly, the T-R path loss cannot reflect the unfairness caused by asymmetric I-R distances as shown in Figure 8(b), where $d_{22} = d_{11}$ while $d_{12} > d_{21}$. In this case, system 2 has higher SINR and outperforms system 1 evidently. Hence system 2 should be encouraged more than system 1 to reduce the transmit power by pricing.

From the observations in the two cases above, we find that only the combination of both the interference level and the T-R path loss can reflect the actual situations properly. Actually, SINR is such a factor that is proportional to the level of pricing for the fairness between the coexisting systems. Therefore we adopt the pricing coefficient τ_i as linear with SINR such that (10) becomes

$$C_i(p_i) = \lambda_i \gamma_i p_i, \tag{11}$$

where λ_i is a constant pricing coefficient with the units of bit/J, γ_i denotes the SINR of link i as

$$\gamma_i = \frac{p_i h_{ii}}{\sum_{j \neq i} p_j h_{ij} \eta_{ij} + \sigma^2}, \tag{12}$$

where h_{ii} is the path loss of link i, h_{ij} and η_{ij} are the path loss and the coupled power factor from the transmitter of link j to the receiver of link i, and σ^2 is the background thermal noise power. Since γ_i is also a linear function of p_j according to (12), the pricing function in (11) is essentially *quadric* with respect to p_j. This is distinguished from the existing linear approaches.

When we consider the system heterogeneity, since R_i and $f_i(\mathbf{p})$ are different in DS and MB-OFDM systems as mentioned previously, the pricing coefficient λ_i should also be different for compensation. Basically, DS UWB outperforms MB-OFDM UWB with the same SINR, λ_i for DS UWB is selected larger (see detailed discussion in Section 4.4).

From (7), (8), and (11), we reform the net utility function of GUTPC as

$$U_i(\mathbf{p}) = R_i f_i(\mathbf{p}) - \lambda_i \gamma_i p_i. \tag{13}$$

Suppose there are totally N coexisting links, then the target of each link i under GUTPC is to maximize its own net utility function by tuning its transmit power, that is,

$$\max U_i(\mathbf{p}) \quad \forall i = 1, 2, \ldots, N. \tag{14}$$

Since R_i, p_i, $f_i(\mathbf{p})$, and λ_i are known to link i, while γ_i can also be available through certain PHY mechanisms such as the link quality indicator [27], the algorithm of GUTPC targeting at (14) can be deployed in a noncooperative way as desired.

4.2. *Feasibility of GUTPC*

Firstly, we define the *infeasible condition* deduced from the property of net utility when the links are turned off due to severe interference. Then the *feasible condition* under GUTPC is defined for both cases with and without maximum power constraint.

For the sake of convenience, we deduce U_i as the function of the γ_i from (13). Comparing (12) with (5), we have $\gamma_b = \mu_i \gamma_i$, where $\mu_i = B_i/(R_i L_i)$ is a constant that covers both the system processing gain and the implementation impairments. Thus, given the packet length k, the goodput V_i as the function of γ_i according to (6), (8), and (9) is

$$V_i(\gamma_i) = R_i f_i(\gamma_i) = R_i \left(1 - \frac{1}{2}\,\mathrm{erfc}\left(\frac{1}{\beta_i}(\mu_i \gamma_i)^{1/\alpha_i}\right)\right)^k. \tag{15}$$

Let $\mathbf{p}_{-i}$ denote the power vector of all the other links except link i, and let $Q_i(\mathbf{p}_{-i}) = \sum_{j \neq i} p_j h_{ij} \eta_{ij} + \sigma^2$ denote the sum of interference and noise power, then according to (12), the pricing function in (11) can be transformed as

$$C_i(\gamma_i) = \lambda_i \frac{Q_i(\mathbf{p}_{-i})}{h_{ii}} \gamma_i^2 = \xi_i \gamma_i^2, \tag{16}$$

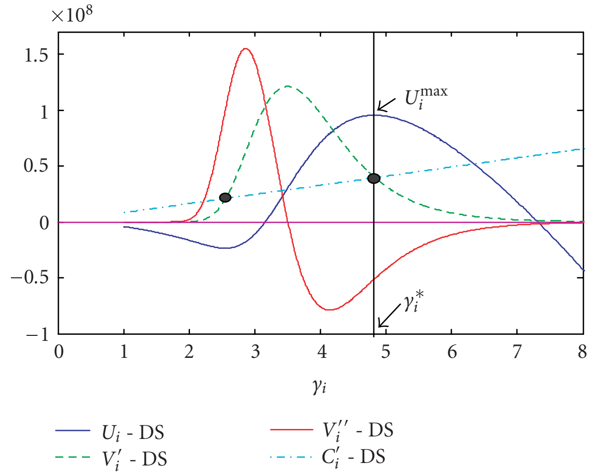

FIGURE 9: Net utility and the derivatives of goodput and price.

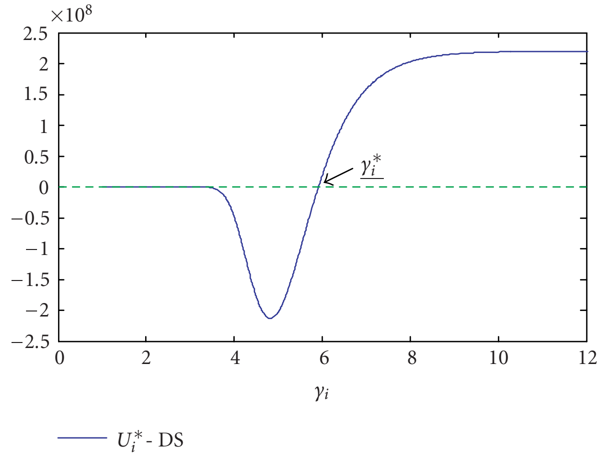

FIGURE 10: U_i^*-net utility achieved at γ_i^*.

where $\xi_i = \lambda_i Q_i(\mathbf{p}_{-i})/h_{ii}$ embodies the transmission environment in terms of interference and T-R path loss.

From (15), (16) we have

$$U_i(\gamma_i) = V_i(\gamma_i) - C_i(\gamma_i) = R_i\left(1 - \frac{1}{2}\operatorname{erfc}\left(\frac{(\mu_i\gamma_i)^{1/\alpha_i}}{\beta_i}\right)\right)^k - \xi_i\gamma_i^2. \quad (17)$$

Based on (17), the necessary condition to maximize U_i is

$$\frac{dU_i}{d\gamma_i} = V_i'(\gamma_i) - C_i'(\gamma_i) = V_i'(\gamma_i) - 2\xi_i\gamma_i = 0, \quad (18)$$

that is,

$$\frac{V_i'(\gamma_i)}{\gamma_i} = 2\xi_i, \quad (19)$$

where V_i' is the first-order derivative of V_i.

By drawing V_i', V_i'' (the second-order derivative of V_i), C_i' (the first-order derivative of C_i), and U_i in Figure 9, we observe that there are two intersections between V_i' and C_i'. Since C_i is convex with respect to γ_i, the maximum of U_i should be achieved at the right-most intersection in the concave part of V_i, that is, $\gamma_i \in \Omega$ such that $V_i'' < 0$. Let $g(\gamma_i) = V_i'(\gamma_i)/\gamma_i$ which is defined on Ω, then we have the optimal SINR γ_i^* from (19) as

$$\gamma_i^* = g^{-1}(2\xi_i), \quad (20)$$

where $g^{-1}(\cdot)$ denotes the inverse function of $g(\cdot)$. From (17) and (19), the net utility U_i achieved at γ_I^* is

$$U_i^* = V_i(\gamma_i^*) - \xi_i\gamma_i^{*2} = V_i(\gamma_i^*) - \frac{V_i'(\gamma_i^*)\gamma_i^*}{2}. \quad (21)$$

By plotting U_i^* in Figure 10, we can see that the maximum of U_i equals U_i^* if and only if $\gamma_i^* > \underline{\gamma}_i^*$. Further, γ_i^* decreases when the transmission environment is getting worse, since $g^{-1}(\cdot)$ is a decreasing function of ξ_i because $g(\gamma_i)$ decreases in $\gamma_i \in \Omega$. When $\gamma_i^* \le \underline{\gamma}_i^*$, the optimal γ_i maximizing U_i can only be zero since U_i approaches zero asymptotically when γ_i approaches zero (since the packet size is very large, i.e., $k = 8192$, in this context), so the best choice of link i is to target its SINR at zero, that is, turn off its transmit power. We define this situation as the *infeasible situation* under GUTPC.

Correspondingly, the *feasible condition* under GUTPC is defined as there exists a component-wise positive power vector $\mathbf{p} = [p_1, p_2, \ldots, p_N]^T$ such that $\gamma_i = \gamma_i^* > \underline{\gamma}_i^*$ for any link i. Here $\underline{\gamma}_i^*$ is the *turn-off point* inherently determined by the goodput function V_i according to (21).

According to (12), we can write the *feasible condition* as

$$\gamma_i = \frac{p_i h_{ii}}{\sum_{j\neq i} p_j h_{ij}\eta_{ij} + \sigma^2} > \underline{\gamma}_i^*, \quad p_i > 0, \quad \forall i = 1, 2, \ldots, N, \quad (22)$$

which can also be translated into the matrix form as

$$(\mathbf{I} - \mathbf{F})\mathbf{p} > \mathbf{\Gamma}, \quad (23)$$

where $\mathbf{I}$ is the identity matrix, $\mathbf{\Gamma}_i = \underline{\gamma}_i^*\sigma^2/h_{ii}$, $\mathbf{F}_{ij} = \underline{\gamma}_i^* h_{ij}\eta_{ij}/h_{ii}$ if $i \neq j$ while $\mathbf{F}_{ii} = 0$. Thus the *feasible condition* is equivalent to having a component-wise positive solution of $\mathbf{p}$ for (23). According to [28], this holds, if and only if, the *Perron-Frobenius* eigenvalue of $\mathbf{F}$ is less than 1.

Furthermore, for a practical coexistence scenario, we should also consider the power constrains: the maximum transmit power is constrained to $p_{\max}$(-9.9 dBm) in both UWB systems. Under the *feasible condition* defined above, the optimal choice of any link i is to target its SINR at γ_i^*. Accordingly, the optimal transmit power p_i^* by (12), (19), and (20) is

$$p_i^* = \frac{\xi_i g^{-1}(2\xi_i)}{\lambda_i} = \frac{V_i'(\gamma_i^*)}{(2\lambda_i)}. \quad (24)$$

Since V_i' decreases in $\gamma_i^* \in \Omega$ while γ_i^* decreases in ξ_i, p_i^* monotonously increases in ξ_i, thus the optimal transmit power resulted from (24) may be unreachable under the constraint of $p_i \leq p_{\max}$ when the transmission environment becomes worse. Nevertheless, if λ_i is large enough, that is,

$$\lambda_i \geq \frac{V_i'(\underline{\gamma}_i^*)}{(2p_{\max})}, \quad (25)$$

then p_i^* can be always achievable (i.e., $p_i^* \leq p_{\max}$) when the *feasible condition* is satisfied. Thus, (25) generalizes the *feasible condition* of (23) for both maximum transmit power constrained and unconstrained situations.

4.3. Convergence of GUTPC

According to [10], the convergence of a *standard power control* is guaranteed with synchronous or asynchronous iterative algorithms from any initial power vector. Here we prove the convergence of GUTPC by showing that it is a *standard power control* under the *feasible condition*.

Define $I_i(\mathbf{p}) = p_i^*$ in (24) as the *interference function* [10] of link i, then the iteration of GUTPC can be written as

$$\mathbf{p}(t+1) = I(\mathbf{p}(t)), \quad (26)$$

where $I(\mathbf{p}) = [I_1(\mathbf{p}), I_2(\mathbf{p}), \ldots, I_N(\mathbf{p})]^T$. Under the *feasible condition*, (26) can be proved to satisfy the necessary and sufficient conditions of a *standard power control* [10]:

(i) positivity: $I(\mathbf{p}) > 0$;
(ii) monotonicity: if $\mathbf{p}' \geq \mathbf{p}$, then $I(\mathbf{p}') \geq I(\mathbf{p})$;
(iii) scalability: for all $\omega > 1$, $\omega I(\mathbf{p}) > I(\omega\mathbf{p})$.

Firstly, the positivity of GUTPC is guaranteed by the *feasible condition* where no link is turned off. Secondly, since $I_i(\mathbf{p}) = p_i^*$ increases with the increasing $\xi_i = \lambda_i Q_i(\mathbf{p}_{-i})/h_{ii}$ as discussed previously, it also increases with $\mathbf{p}$ given λ_i, h_{ii}, and h_{ji}. Hence, the monotonicity is guaranteed. Finally, since

$$\begin{aligned} Q_i(\mathbf{p}_{-i}) < Q_i(\omega\mathbf{p}_{-i}) &= \sum_{j\neq i} \omega p_j h_{ij}\eta_{ij} + \sigma^2 \\ &< \sum_{j\neq i} \omega p_j h_{ij}\eta_{ij} + \omega\sigma^2 = \omega Q_i(\mathbf{p}_{-i}), \end{aligned} \quad (27)$$

and $g^{-1}(\cdot)$ is decreasing in ξ_i, according to (24) we have

$$\begin{aligned} I_i(\omega\mathbf{p}) &= \frac{Q_i(\omega\mathbf{p}_{-i})}{h_{ii}} g^{-1}\left(2\lambda_i \frac{Q_i(\omega\mathbf{p}_{-i})}{h_{ii}}\right) \\ &< \frac{Q_i(\omega\mathbf{p}_{-i})}{h_{ii}} g^{-1}\left(2\lambda_i \frac{Q_i(\mathbf{p}_{-i})}{h_{ii}}\right) < \omega I_i(\mathbf{p}). \end{aligned} \quad (28)$$

Thus the scalability is satisfied. Consequently, GUTPC is *standard*, thereby converges under its *feasible condition*.

In a practical environment, the estimation of SINR and power might be inaccurate and fluctuating due to channel fading or hardware implementation issues, thus an interference averaging approach can be adopt in GUTPC, that is,

$$\mathbf{p}(t+1) = \exp\left(\varepsilon \ln\left(\mathbf{p}(t)\right) + (1-\varepsilon)\ln\left(I(\mathbf{p}(t))\right)\right), \quad (29)$$

where $0 < \varepsilon < 1$ is a forgetting factor for previous iteration. According to [10], (29) is still *standard*, thus converges.

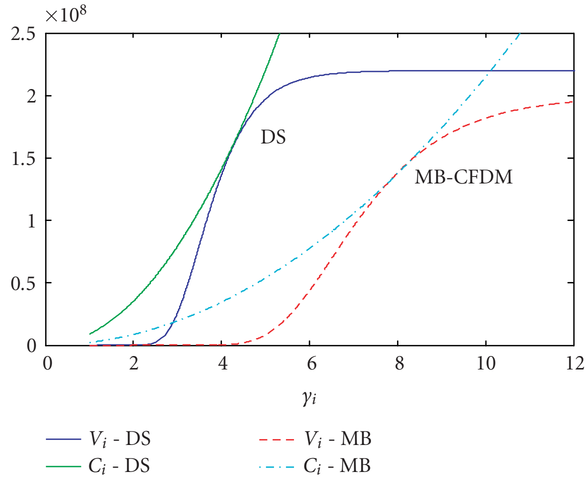

Figure 11: Turnoff condition of MB-OFDM and DS UWB.

4.4. Turnoff fairness and the choice of λ_i

Under the algorithm of GUTPC, all the functions and variables in the net utility (13) are inherently determined or measurable except the pricing coefficient λ_i, which can be adjusted based on the requirement. Next we discuss the choice of λ_i in terms of both fairness and efficiency.

On one hand, different λ_i reflects different level of pricing and leads to different convergent outcome under GUTPC. To be fair between the heterogeneous coexisting systems, here we propose *turnoff fairness* as the basic criterion for the choice of λ_i. *Turnoff fairness* is defined as the coexisting systems would be turned off under the same transmission environment in terms of interference and T-R path loss. The detailed explanation is given below.

Basically, (25) provides a guide for the choice of λ_i to generalize the *feasible condition* under GUTPC. Let $\underline{\lambda}_i$ be the minimum λ_i that (25) holds. When λ_i increases from $\underline{\lambda}_i$, γ_i^* decreases according to (20), then an originally *feasible* problem may become *infeasible* when $\gamma_i^* \leq \underline{\gamma}_I^*$. This means that the increasing λ_i makes the same situation severer to the victim system, which is more likely to be turned off. In this sense, we intend to choose λ_i fairly between the coexisting systems considering their heterogeneity. As seen from Figure 11, the *turnoff point* ($\gamma_i^* = \underline{\gamma}_i^*$) should be reached by the heterogeneous UWB systems under the same transmission environment (i.e., $Q_i(\mathbf{p}_{-i})/h_{ii}$). According to (19), we have

$$\frac{V_i'(\underline{\gamma}_i^*)}{\underline{\gamma}_i^*} = \frac{2\lambda_i Q_i(\mathbf{p}_{-i})}{h_{ii}}. \quad (30)$$

Thus, the *turnoff fairness* can be achieved by setting a proper ratio ρ between the pricing coefficients of the coexisting systems as

$$\rho = \frac{\lambda_{\mathrm{MB}}}{\lambda_{\mathrm{DS}}} = \frac{\underline{\gamma}_{\mathrm{DS}}^* V_{\mathrm{MB}}'(\underline{\gamma}_{\mathrm{MB}}^*)}{\underline{\gamma}_{\mathrm{MB}}^* V_{\mathrm{DS}}'(\underline{\gamma}_{\mathrm{DS}}^*)}, \quad (31)$$

which is totally determined by the goodput function of each system. If only (31) is satisfied, we call the coexisting systems *turnoff fair*.

Considering the generalized condition in (25), initially we can set the pricing coefficient λ_i of each system as

$$\lambda_{\text{MB}}^{\text{init}} = \max\{\underline{\lambda_{\text{MB}}}, \rho\underline{\lambda_{\text{DS}}}\},$$
$$\lambda_{\text{DS}}^{\text{init}} = \max\left\{\frac{\underline{\lambda_{\text{MB}}}}{\rho}, \underline{\lambda_{\text{DS}}}\right\}, \quad (32)$$

where $\underline{\lambda_{\text{MB}}}$ and $\underline{\lambda_{\text{DS}}}$ are the $\underline{\lambda_i}$ of MB-OFDM and DS systems following (25), respectively. By (32), we get the *turnoff fair* setup of the pricing coefficient λ_i while satisfying the generalized *feasible condition*.

However, (25) is only sufficient for generalizing the *feasible condition* while not necessary for a given coexistence scenario. It could make the choice of λ_i inefficient by (32). Specifically, if λ_i is large enough, the convergent power vector $\mathbf{p}$ can be component-wise less than $p_{\max}$ since p_i^* is decreasing in λ_i according to (24). Such a result is *Pareto inefficient* according to [9, Theorem 1]. Actually, we can tune down λ_i of each system simultaneously by the same scale until λ_i^{opt} such that the convergent power p_i^* of any system firstly reaches $p_{\max}$. (Practically, if the common signaling mode (CSM) [29] is supported by the coexisting systems, this can be implemented by certain negotiations between the coexisting systems.) In this way, *Pareto optimal* is achieved along with *turnoff fairness*. Such outcome also implies *max-min fairness* [30] in a certain sense since the system that firstly reaches $p_{\max}$ has the poorest goodput because higher p_i^* is associated with lower target SINR γ_i^* following (24). Actually the *turnoff fairness* outcome with λ_i^{opt} closely approximates the *proportional fairness* result (though cannot be strictly proved) as will be seen from the evaluation results in the next section.

5. PERFORMANCE EVALUATION

In this section, we evaluate the performance of GUTPC applied in the UWB coexistence scenarios. All the evaluated cases are selected *feasible* under GUTPC, since the adaptiveness of GUTPC to the *infeasible* situation is similar to that in [25]. The performance improvement in terms of *total goodput* and *fairness* by GUTPC is shown by comparing with the coexistence result without power control and the *max-min fair* and *proportional fair* outcomes. The typical cases mentioned in Figure 8 are evaluated at first. Then a statistical result of 100 random network cases is presented to show the general performance of GUTPC under more realistic and complicated scenarios. Above all, we explain the simulation setups.

5.1. Parameter and metric selection

In all the simulations, the transmit power is limited below $p_{\max} = -9.9$ dBm. The result without power control is the outcome by each system transmitting at $p_{\max}$. For GUTPC and the *max-min fair* and *proportional fair* results, 1 dB step size is selected for power tuning, which can be resolved as per IEEE 802.15.3 MAC standard [27]. Additionally, 0.2 dB step size is also investigated to see the quantizing effects of the power level on the convergent results.

Total goodput and *fairness* are taken as two primary metrics, while *total power* is investigated as well. They are all evaluated at the equilibrium stage. It is worth noting that *fairness* is defined as the squared cosine of the angle between the resulting goodput vector and the *max-min fair* goodput vector, which theoretically should be component-wise equal in a wireless ad hoc network [31]. However, in our practical coexistence problem, this may not be achievable due to the discrete power levels. Instead, we approximate the *max-min fair* outcome by the goodput vector angularly closest to the theoretical result. In case multiple results with the same *fairness* exist, the one with largest *total goodput* is selected. The *proportional fair* outcome is selected as the goodput vector with the maximal component-wise logarithmic sum according to its definition [31]. Both the *max-min fair* and *proportional fair* results are achieved by exhaustive search.

5.2. Numerical results

Firstly, we investigate the typical cases discussed in Figure 8 and illustrate the evaluation results of case (a) in Figure 12 for example (the results of case (b) are quite similar). In case (a), we set system 1 as DS UWB, system 2 as MB-OFDM UWB. We fix $d_{11} = 1.2$ m, $d_{22} = 4$ m, while vary the vertical distance between the two parallel links to see the effects under different interference conditions. The results at very short "inter-link distance" (< 6.8 m) are not demonstrated since those are actually *infeasible* under GUTPC when one of the coexisting systems would be turned off.

From Figure 12(a), we can see that the *fairness* performance of GUTPC with the initial pricing coefficients $\lambda_{\text{MB}}^{\text{init}}$ and $\lambda_{\text{DS}}^{\text{init}}$ is very close to the *proportional fair* outcome at all distances. This is attributed to the SINR-based pricing function which takes care of the *fairness* of goodput by considering both T-R distance and interference level. Although the *max-min fair* outcome has slight advantage in *fairness* at short coexisting distance, it is actually traded from the goodput efficiency as seen in Figure 12(b). With the same λ_i^{init}, GUTPC greatly improves the efficiency of the coexisting systems in terms of *total goodput*. Under many circumstances, GUTPC even beat the *max-min fair* results in *total goodput* due to the inefficiency of *max-min fairness* caused by the system heterogeneity. Note that the *total goodput* of GUTPC with λ_i^{init} has zigzags along the vertical distance. It can be explained as the quantizing effect of the tunable power level as shown in Figure 12(b) by plotting the smoother curve with a smaller (0.2 dB) power step size. After all, with the optimal pricing coefficient λ_i^{opt}, GUTPC can almost exactly matches the *proportional fair* results not only in *fairness*, but also in *total goodput* and *total power* performances. Although the power consumption is not considered critical in the UWB coexistence problem, it is desirable that GUTPC saves energy to a great extent as seen in Figure 12(c). However, the lowest *total power* consumption achieved by GUTPC with λ_i^{init} is traded from the *total goodput* efficiency comparing to the results with λ_i^{opt}.

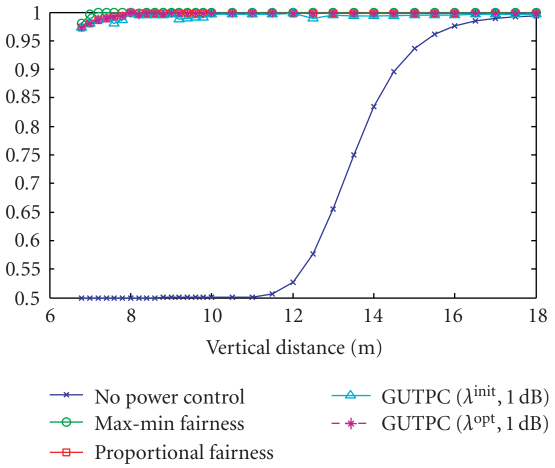

(a) Fairness performance

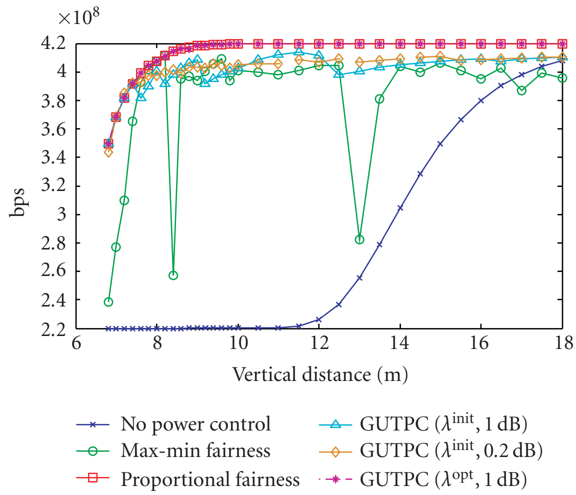

(b) Total goodput performance

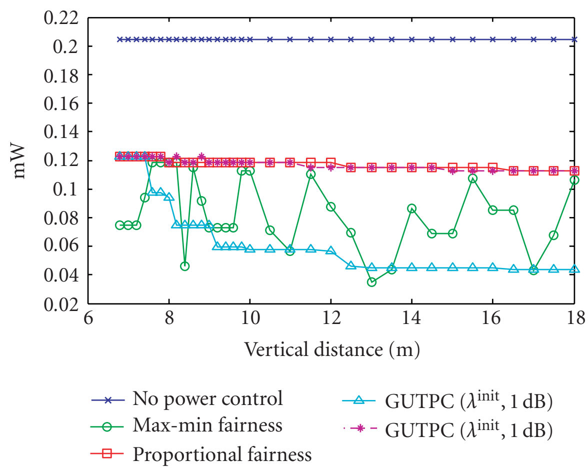

(c) Total power performance

Figure 12

Next, we investigate the performance of GUTPC in the random network coexistence cases of the heterogeneous UWB systems. Without losing generality, we build a TDMA network with four independent links for each system. Both systems have 128 time-slots per super-frame and 1 dB power control step. The statistical results over 100 cases with random network topologies and time-slot allocations are presented in Figure 13. We focus only on the cases in which the coexistence problem is relatively serious, that is, the *total goodput* without power control is less than 85% of the maximum *total goodput* (420 Mbps) of the coexisting systems. From the statistical results we can see that GUTPC with λ_I^{opt} still approximate the *proportional fairness* closely under such general and practical circumstances. Furthermore, although GUTPC with λ_i^{init} experiences certain deterioration in *total goodput* comparing to *proportional fairness*, it keeps remarkable *fairness* performance and improves the goodput of the coexisting systems better than the *max-min fair* outcome. Being consistent with the results in Figure 12, all these observations show that the proposed GUTPC algorithm is reliable and stable which is further manifested by the standard deviation results in Figure 13.

Conclusively, GUPTC is an effective, efficient, and fair TPC algorithm for the interference mitigation between the heterogeneous UWB systems under various coexisting scenarios. Actually, it can approximate the *proportional fair* criterion quite well thanks to its adaptive SINR-based pricing function with well-selected pricing coefficient that incorporates the heterogeneity.

6. CONCLUSION

In this paper we analyze the coexistence of two UWB systems, MB-OFDM UWB and DS UWB, for high-speed WPAN through PHY Monte Carlo simulation. Our simulation results demonstrate the severe interference in the coexistence scenarios of the two UWB systems, which motivates our proposal for interference mitigation by power control. We

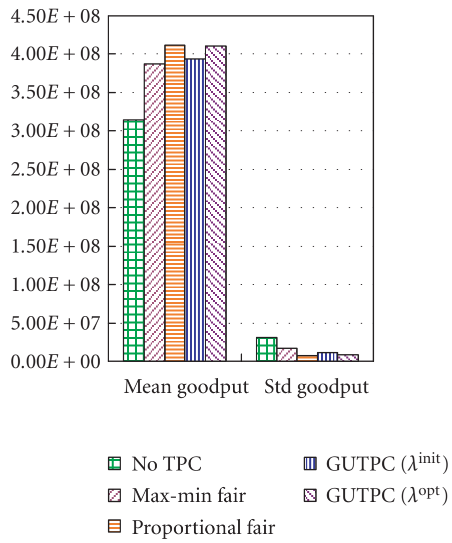

(a) Fairness performance

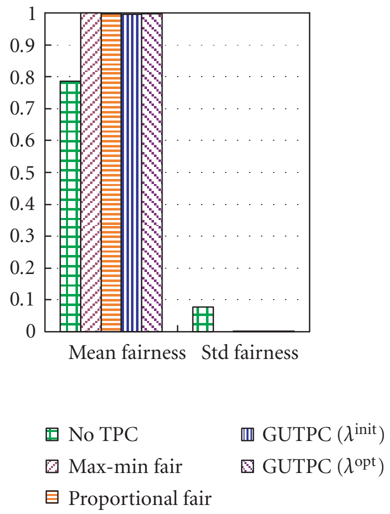

(b) Total goodput performance

FIGURE 13: Statistical results over 100 random network cases.

propose a power control algorithm named GUTPC for the coexistence scenario. The novelty in GUTPC lies in the pricing function where SINR is introduced to represent the potential mutual impact between the coexisting systems. In addition, the asymmetric impact due to the heterogeneity is considered for fairness, resulting in the differentiated pricing coefficients. The feasibility of GUTPC is analyzed with and without maximum transmit power constraint, and the convergence is proved by showing that it follows a *standard power control* when feasible. Through simulation results, we observe that GUTPC achieves high performance in terms of both *total goodput* and *fairness* for the heterogeneous UWB coexistence and approximates *proportional fairness* closely with the optimal pricing coefficient.

REFERENCES

[1] http://www.uwbforum.org, January 2006.

[2] M. Hämäläinen, J. Saloranta, J.-P. Mäkelä, I. Oppermann, and T. Patana, "Ultra-wideband signal impact on the performances of IEEE 802.11b and bluetooth networks," *International Journal of Wireless Information Networks*, vol. 10, no. 4, pp. 201–210, 2003.

[3] D. K. Borah, R. Jana, and A. Stamoulis, "Performance evaluation of IEEE 802.11a wireless LANs in the presence of ultra-wideband interference," *IEEE Wireless Communications and Networking*, vol. 1, pp. 83–87, 2003.

[4] J. Bellorado, S. S. Ghassemzadeh, L. J. Greenstein, T. Sveinsson, and V. Tarokh, "Coexistence of ultra-wideband systems with IEEE-802.1la wireless LANs," in *Proceedings of IEEE Global Telecommunications Conference (GLOBECOM '03)*, vol. 1, pp. 410–414, San Francisco, Calif, USA, December 2003.

[5] R. Giuliano, G. Guidoni, F. Mazzenga, and F. Vatalaro, "On the coexistence of UWB with fixed wireless access systems," in *Proceedings of the 8th International Conference on Personal Wireless Communications (PWC '03)*, vol. 2775 of *Lecture Notes in Computer Science*, pp. 101–113, Venice, Italy, September 2003.

[6] M. Hämäläinen, V. Hovinen, R. Tesi, J. H. J. Iinatti, and M. Latva-Aho, "On the UWB system coexistence with GSM900, UMTS/WCDMA, and GPS," *IEEE Journal on Selected Areas in Communications*, vol. 20, no. 9, pp. 1712–1721, 2002.

[7] C. A. Corral, S. Emami, and G. Rasor, "In-band interference of multi-band OFDM systems," in *IEEE International Symposium on Spread Spectrum Techniques and Applications*, pp. 793–796, Leura, Australia, August-September 2004.

[8] K. Ohno, T. Ikebe, and T. Ikegami, "A proposal for an interference mitigation technique facilitating the coexistence of biphase UWB and other wideband systems," in *Proceedings of International Workshop on Joint UWBST & IWUWBS*, pp. 50–54, Kyoto, Japan, May 2004.

[9] C. W. Sung and W. S. Wong, "A noncooperative power control game for multirate CDMA data networks," *IEEE Transactions on Wireless Communications*, vol. 2, no. 1, pp. 186–194, 2003.

[10] R. D. Yates, "A framework for uplink power control in cellular radio systems," *IEEE Journal on Selected Areas in Communications*, vol. 13, no. 7, pp. 1341–1347, 1995.

[11] A. Batra, J. Balakrishnan, A. Dabakand, et al., "Multi-band OFDM Physical Layer Proposal for IEEE 802.15 Task Group 3a," IEEE P802.15-03/268r3, March 2004.

[12] R. Fisher, R. Kohno, M. Mc Laughlin, et al., "DS-UWB Physical Layer Submission to 802.15 Task Group 3a," IEEE P802.15-04/0137r4, January 2005.

[13] MultiBOFDM Alliance SIG, "MultiBand OFDM Physical Layer Proposal for IEEE 802.15 Task Group 3a," http://www.multibandofdm.org/presentations.html, September 2004.

[14] A. Batra, J. Balakrishnan, G. R. Aiello, J. R. Foerster, and A. Dabak, "Design of a multiband OFDM system for realistic UWB channel environments," *IEEE Transactions on Microwave Theory and Techniques*, vol. 52, no. 9, part I, pp. 2123–2138, 2004.

[15] B. Muquet, Z. Wang, G. B. Giannakis, M. De Courville, and P. Duhamel, "Cyclic prefixing or zero padding for wireless multicarrier transmissions?" *IEEE Transactions on Communications*, vol. 50, no. 12, pp. 2136–2148, 2002.

[16] M. Suzuki, C. Fujita, M. Yotsuya, K. Takamura, and T. Usui, "Techniques for MB-OFDM improvement," IEEE 15-03-0337-01-003a, September 2003.

[17] M. Welborn, "DS-UWB Responses to TG3a Voter NO Comments," IEEE P802.15-05/0050r2, January 2005.

[18] S. S. Ghassemzadeh, L. Greenstein, O. Shin, and V. Tarokh, "Parameter assumptions for the simulation of the proposed 802.15.3a PHYs," DCN # 15-04-0488-00-003a, September 2004.

[19] M. Mc Laughlin, "Detailed DS-UWB simulation results," IEEE P802.15-04/0483r5, November 2004.

[20] J. G. Proakis, *Digital Communications*, McGraw-Hill, New York, NY, USA, 4th edition, 2001.

[21] R. Fisher, R. Kohno, H. Ogawa, H. Zhang, and K. Takizawa, "Merger#2 Proposal DS-CDMA," IEEE 802.15-03/334r5, November 2003.

[22] J. Foerster, "Channel Modeling Sub-committee Report Final," IEEE P802.15-02/490r1-SG3a, February 2003.

[23] J. Ellis, K. Siwiak, and R. Roberts, "TG3a Technical Requirements," IEEE P802.15-03/030r0, December 2002.

[24] J. McCorkle, "DS-CDMA: The Technology of Choice for UWB," IEEE P802.15-03/277r0, July 2003.

[25] M. Xiao, N. B. Shroff, and E. K. P. Chong, "A utility-based power-control scheme in wireless cellular systems," *IEEE/ACM Transactions on Networking*, vol. 11, no. 2, pp. 210–221, 2003.

[26] C. U. Saraydar, N. B. Mandayam, and D. J. Goodman, "Efficient power control via pricing in wireless data networks," *IEEE Transactions on Communications*, vol. 50, no. 2, pp. 291–303, 2002.

[27] IEEE, "Wireless Medium Access Control (MAC) and Physical Layer (PHY) Specifications for High Rate Wireless Personal Area Networks (WPANs)," IEEE Std 802.15.3TM-2003, September 2003.

[28] D. Mitra, "An asynchoronous distributed algorithm for power control in cellular radio systems," in *Proceedings of 4th Winlab Workshop on Third Generation Wireless Information Network*, pp. 249–257, East Brunswick, NJ, USA, October 1993.

[29] M. Welborn, "Extended Common Signaling Mode," IEEE 802.15-04/341r2, November 2004.

[30] D. P. Bertsekas and R. Gallager, *Data Networks*, Prentice-Hall, Englewood Cliffs, NJ, USA, 2nd edition, 1992.

[31] B. Radunovic and J.-Y. Le Boudec, "Rate performance objectives of multihop wireless networks," *IEEE Transactions on Mobile Computing*, vol. 3, no. 4, pp. 334–349, 2004.

Yongjing Zhang received the B.S. degree in telecommunication engineering from Beijing University of Posts and Telecommunications (BUPT), China, in 2002. He is now working towards the Ph.D. degree at the same university. From December 2003 to July 2004, he was a visiting student in Microsoft Research, Asia, working on the coexistence of heterogeneous ultra-wideband systems. His current research interests include the joint radio resource management, network element management, and dynamic spectrum management of the end-to-end reconfigurable system.

Haitao Wu received his Bachelor degree in telecommunication engineering and his Ph.D. degree in telecommunication and information system, in 1998 and 2003, respectively, both from Beijing University of Posts and Telecommunications (BUPT). He is a Member of the IEEE. In July 2003, he joined Wireless and Networking Group, Microsoft Research Asia (MSRA) as an Associate Researcher. Before that, he has over 30 papers published and 5 patents filed. His research interests are QoS, TCP/IP, P2P, wireless networks, and mobile systems.

Qian Zhang received the B.S., M.S., and Ph.D. degrees from Wuhan University, China, in 1994, 1996, and 1999, respectively, all in computer science. She joined Hong Kong University of Science and Technology in September 2005 as an Associate Professor. Before that, she was in Microsoft Research, Asia, from July 1999, where she was a Research Manager of Wireless and Networking Group. She has published more than 120 refereed papers in international leading journals and conferences. She is the inventor of about 30 pending patents. Her current research interests are in the areas of wireless communications, IP networking, multimedia, P2P overlay, and wireless security. She is the Associate Editor for the IEEE Transactions on Wireless Communications, the IEEE Transactions on Multimedia, and the IEEE Transactions on Vehicular Technologies and Computer Communications. She also served as a Guest Editor for special issue in the IEEE Wireless Communication Magazine and is serving as a Guest Editor for special issue in the IEEE JSAC. She has received TR 100 (MIT Technology Review) World's Top Young Innovator Award. She also received the Best Asia Pacific Young Researcher Award elected by IEEE Communication Society. She received the Best Paper Award in Multimedia Technical Committee (MMTC) of the IEEE Communication Society. She is Chair of QoSIG of the Multimedia Communication Technical Committee of the IEEE Communications Society.

Ping Zhang received the Ph.D. degree from Beijing University of Posts and Telecommunications (BUPT) in 1990, and the M.S. degree from Northwest Polytechnic University in 1986, both in electrical engineering. He was a Postdoctoral Researcher in the PCS Department, Korea Telecom Wireless System Development Center. Currently, he is a Professor of BUPT and Director of Wireless Technology Innovation (WTI) Institute, BUPT. He has also served as the Senior Member of C3G Group, China MOST 863 future mobile communication FuTURE project, Vice-Chairman of World Wireless Research Forum (WWRF), and Member of Vision Committee. He is also invited as the consultant for many domestic and overseas communication companies. He is very active on the international research activity on beyond 3G research activity. He also participated in several European projects such as E2R and MOCCA. Until now, he has published 6 books, around 400 publications in journals and conferences in the area of telecommunications. His main research interests are theory and applications in wireless communication area. He was awarded by the government, of the city of Beijing and Ministry of Information Industry several times for his great contribution to the industry and research activity in China.